

# Persistent river heatwaves are emerging worldwide under climate change

Received: 2 April 2025

Accepted: 18 November 2025

Published online: 06 January 2026

 Check for updates

Yiling Chen<sup>1</sup>, Zhiying Su<sup>1</sup>, R. Iestyn Woolway<sup>2</sup>, Niko Wanders<sup>3</sup>, Sijia Wu<sup>1</sup>,  
Ziwei Huang<sup>1</sup> & Ming Luo<sup>1</sup> ✉

Rivers and the organisms living within them are highly vulnerable to hot thermal extremes. However, very little is known about river heatwaves, consecutive episodes of anomalously high temperature in rivers, and how they may evolve under climate change. Here we show that river heatwaves will become more intense and more persistent globally by the end of the 21<sup>st</sup> century, with some tropical rivers reaching a persistent year-round heatwave state in the early 21<sup>st</sup> century. Under the high-greenhouse-gas-emission scenario (Representative Concentration Pathway 8.5), the average intensity of river heatwaves will increase by ~4.2-fold, and the average duration by ~95-fold, relative to the baseline period (1976–2005). Nearly half of the world's rivers are expected to experience a year-round heatwave state by the 2090 s. Global population exposure to river heatwaves will reach 16.8 billion person-weeks annually, with a disproportionately heavier burden on vulnerable low-income regions, such as the Congo River basin. Emerging persistent river heatwaves may push river ecosystems and aquatic organisms to their resilience limits, causing irreversible changes and widespread impacts.

Rivers provide an efficient network that links terrestrial and marine ecosystems through the transportation of water, energy, and nutrients<sup>1</sup>. River water temperature is a fundamental water variable that regulates physical, chemical, and biological processes within river systems<sup>2</sup>. Extremely high temperatures in rivers can affect water quality and the survival, growth, and distribution of aquatic organisms, impacting ecosystems and human societies<sup>2–4</sup>. Aquatic organisms are susceptible to changes in river temperature, and rising temperatures pose a severe threat to the survival of freshwater fishes<sup>5</sup>, which provide a primary protein source for a large portion of the human population<sup>6</sup>. The increasing exposure of these species to extreme high temperatures may result not only in local extinctions but also threaten fisheries that support the livelihoods of humans in many regions of the world<sup>7</sup>. Higher temperatures reduce dissolved oxygen levels in rivers while increasing the concentration of dissolved organic matter, micro-pollutants, and pathogens<sup>8</sup>. These changes can degrade water quality and metabolism<sup>9</sup>, posing risks to both human health and water

security<sup>10</sup>. As climate change intensifies, river temperatures are likely to rise further<sup>11–13</sup>. Therefore, understanding the long-term dynamics of river water temperatures has become critically urgent for developing strategies to mitigate the risks to ecosystems and societies that depend on river resources.

Previous studies on extreme high temperatures have primarily focused on those in the atmosphere<sup>14–16</sup>, oceans<sup>17,18</sup>, and lakes<sup>19,20</sup>, where positive trends in heatwave frequency and intensity have been well-documented. There is growing evidence that river water temperatures are increasing under climate change<sup>11,12,21</sup>. In comparison, we know much less about heatwaves in rivers and how they might evolve in a warming world<sup>13,22,23</sup>. A river heatwave event can be defined as a period when river water temperature exceeds a local and seasonally varying 90<sup>th</sup> percentile threshold over the historical baseline period (see “Methods” for more details), similar to atmospheric and marine heatwaves<sup>14–18</sup>. The knowledge gap of river heatwaves is of considerable concern, given the high vulnerability of

<sup>1</sup>Guangdong Provincial Key Laboratory of Urbanization and Geo-Simulation, School of Geography and Planning, Sun Yat-sen University, Guangzhou, China.

<sup>2</sup>School of Ocean Sciences, Bangor University, Bangor, UK. <sup>3</sup>Department of Physical Geography, Utrecht University, Utrecht, the Netherlands.

✉ e-mail: [luom38@mail.sysu.edu.cn](mailto:luom38@mail.sysu.edu.cn)

ivers to heat extremes and the ecosystem goods and services that they provide<sup>3,24–26</sup>.

In this study, we present a global assessment of river heatwaves and explore their future changes under different Representative Concentration Pathways (RCPs). We also estimate future population exposure to river heatwaves by integrating projected population data under different Shared Socioeconomic Pathways (SSPs). Our assessment of the spatiotemporal changes in river heatwaves and their potential impacts on humans across scenarios and sectors with different income levels is expected to offer valuable insights for adapting activities and regulations in changing aquatic environments.

## Results

### Historical trends in global river heatwaves

The occurrences and characteristics of river heatwaves are analyzed based on a global bias-corrected dataset of multi-model simulated historical and future streamflow and water temperature at a five arc-minute resolution (~10 km at the equator) from 1976 to 2099<sup>11</sup> (see “Methods”). Using an additional reanalysis yields a similar historical pattern of global river heatwaves (see Methods). For each river grid cell, a river heatwave event is defined as a consecutive period during

which weekly river mean water temperature exceeds the 90<sup>th</sup> percentile threshold (Supplementary Fig. 1), which is calculated over the 30-year historical baseline period of 1976–2005 (see “Methods” for more details). On average, global rivers experience 2.19 river heatwave events per year during the historic period (Supplementary Fig. 2 and Supplementary Table 1). These events exhibit an average intensity (i.e., temperature exceedance relative to the threshold) of 0.64 °C and an average duration of 2.27 weeks (Fig. 1 and Supplementary Table 1).

The river heatwave characteristics vary across geographic and climatic zones (Fig. 1 and Supplementary Fig. 3). The highest frequency of river heatwave events occurs in arid and temperate regions (2.49 and 2.51 events per year, respectively), while cold climatic zones experience the fewest river heatwave occurrences (1.79 events per year). In terms of intensity, rivers in cold and arid zones exhibit the highest temperature exceedances, with average river heatwave intensities of 0.82 °C and 0.71 °C (Fig. 1a), respectively, likely due to stronger temperature variations in the overlying atmosphere in these regions (Supplementary Fig. 4). There is an increase in heatwave intensity with an increase in absolute latitude. The average duration of river heatwaves tends to decrease with increasing latitude (Fig. 1b), with rivers around 5°N having more persistent river heatwaves (with an average

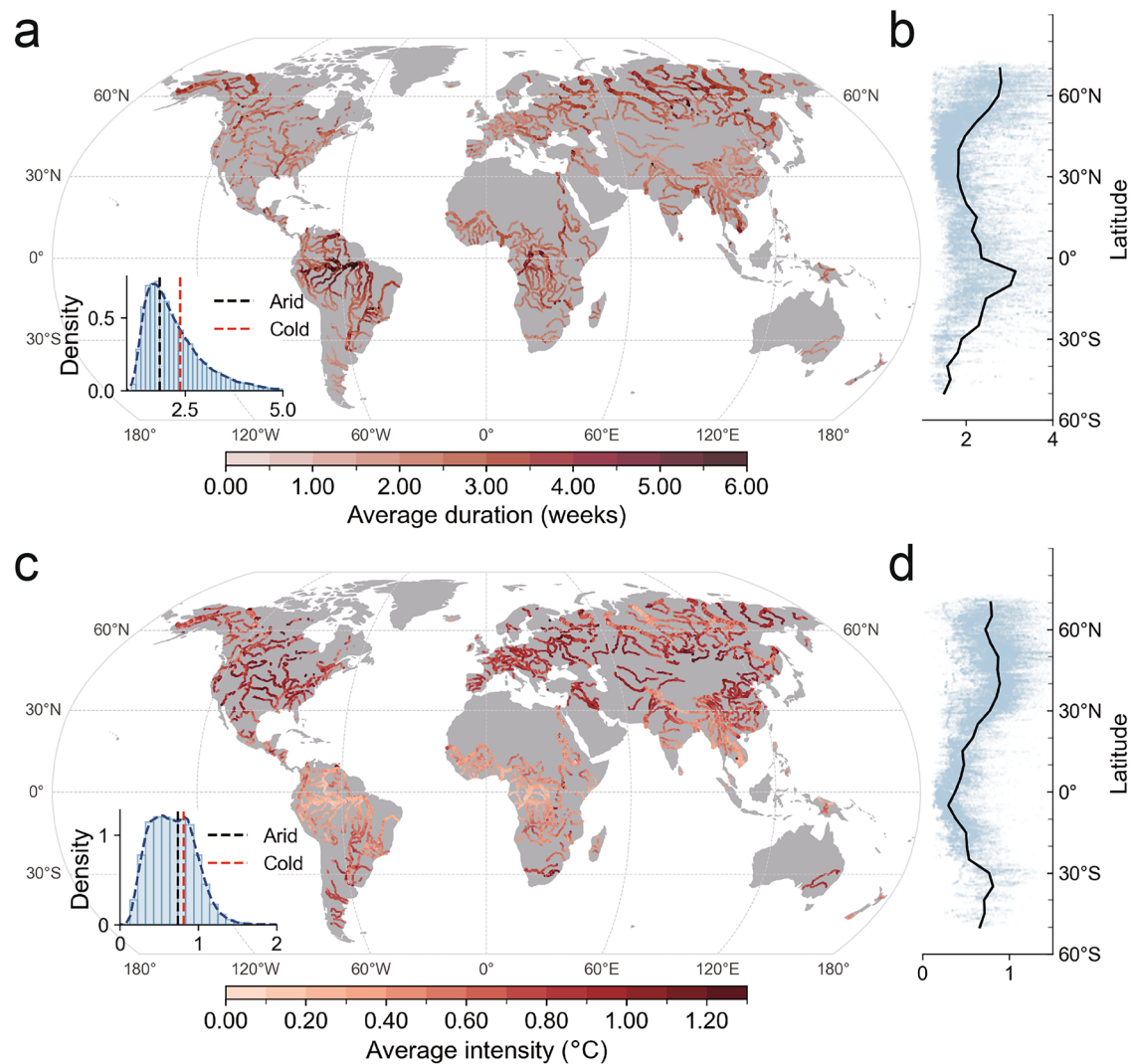


**Fig. 1 | Historical mean state of river heatwaves.** Spatial distribution of the average duration per event (a) and average intensity (c) of global river heatwaves during the historical period of 1976–2005. The density distributions are shown in the embedded charts of (a and c), with black and red dashed vertical lines

representing the mean values for arid and cold zones, respectively. Latitudinal averages of river heatwave duration (b) and intensity (d), with blue scatter points representing the averages for individual rivers. Basemaps in a and c are from Natural Earth (<https://www.naturalearthdata.com>).

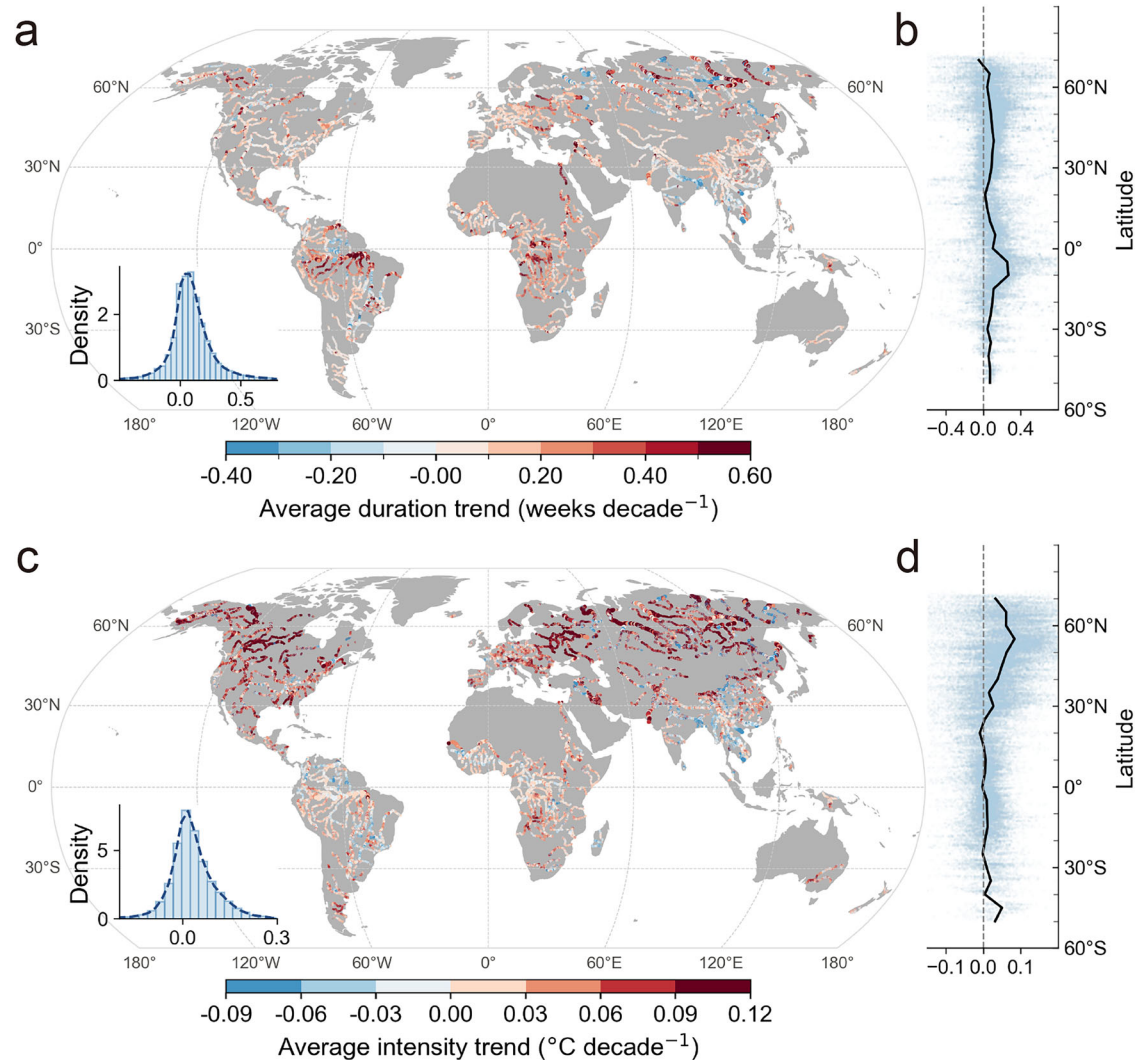


**Fig. 2 | Historical trends in river heatwaves.** Spatial distribution of the historical trends in the average duration (a) and intensity (c) of global river heatwaves from 1976 to 2005, with their density distributions shown in the embedded charts of (a, c). The historical long-term trends are estimated by Theil-Sen's slope estimator.

Latitudinal averages of the long-term trends in river heatwave duration (b) and intensity (d), with blue scatter points representing the trends for individual rivers. Basemaps in a and c are from Natural Earth (<https://www.naturalearthdata.com>).

duration of -3.20 weeks). These spatial patterns are somewhat similar to those for atmospheric heatwaves (Supplementary Fig. 5), suggesting a close relationship between river heatwaves and atmospheric heat extremes<sup>22</sup>. River heatwaves also exhibit relatively long durations at high latitudes (i.e., an average of 2.75 weeks in the north of 65°N), similar to the latitudinal distributions of marine heatwaves<sup>27,28</sup> and atmospheric heatwaves in the permafrost Arctic<sup>29</sup>, which is partially attributed to the shrinking of snow cover and sea ice<sup>30–32</sup>. For different basins, the mainstem river regions, such as the central Amazon basin, exhibit more persistent heatwaves, whereas surrounding tributaries show shorter durations. These differences in heatwave duration within the same basin may be related to different river discharges<sup>22</sup>.

The average intensity of river heatwaves has increased during the historical period, at a rate of 0.02 °C per decade ( $p$ -value < 0.01), and their duration has prolonged by 0.09 weeks per decade ( $p$ -value < 0.01). Changes in the duration and intensity of river heatwaves are closely linked to the increase in river water temperature (Supplementary Fig. 6), which has increased at a rate of 0.20 °C/decade ( $p$ -value < 0.01) from 1976 to 2005. The greatest increase in river heatwave duration appears in tropical low-latitude regions (Fig. 2a and Supplementary Table 2). In contrast, the most pronounced increases in the intensity of river heatwaves are seen at high latitudes, including the

Saint Lawrence, Columbia, Colorado, Rhine, and Danube river basins (Fig. 2c and Supplementary Table 2), corresponding to higher rates of river water temperature trends in these regions (Supplementary Fig. 7). Among global major basins, the fastest prolonged trends in river heatwave duration are seen in the Amazon, Nile, Danube, and Congo river basins. The strongest increasing trends in heatwave frequency are observed in the Rhine, Elbe, Amazon, and Congo river basins (Supplementary Table 2).

### Future trends in global river heatwaves

The duration, intensity, and frequency of river heatwaves are projected to increase from the historical (1976–2005) to future (2006–2099) periods (Fig. 3 and Supplementary Figs. 8–9). Here, future changes are evaluated under four greenhouse-gas-emission scenarios (i.e., RCPs). Except for the low-emission scenarios (RCP 2.6), all scenarios show increasing trends in the river heatwave metrics. The annual frequency of river heatwaves is projected to decrease after 2060, suggesting that some river heatwave events may last multiple years (Supplementary Fig. 9). The decreases in the river heatwave frequency are the earliest and most pronounced under RCP 8.5, reflecting a shift in river heatwaves towards fewer but more prolonged events.

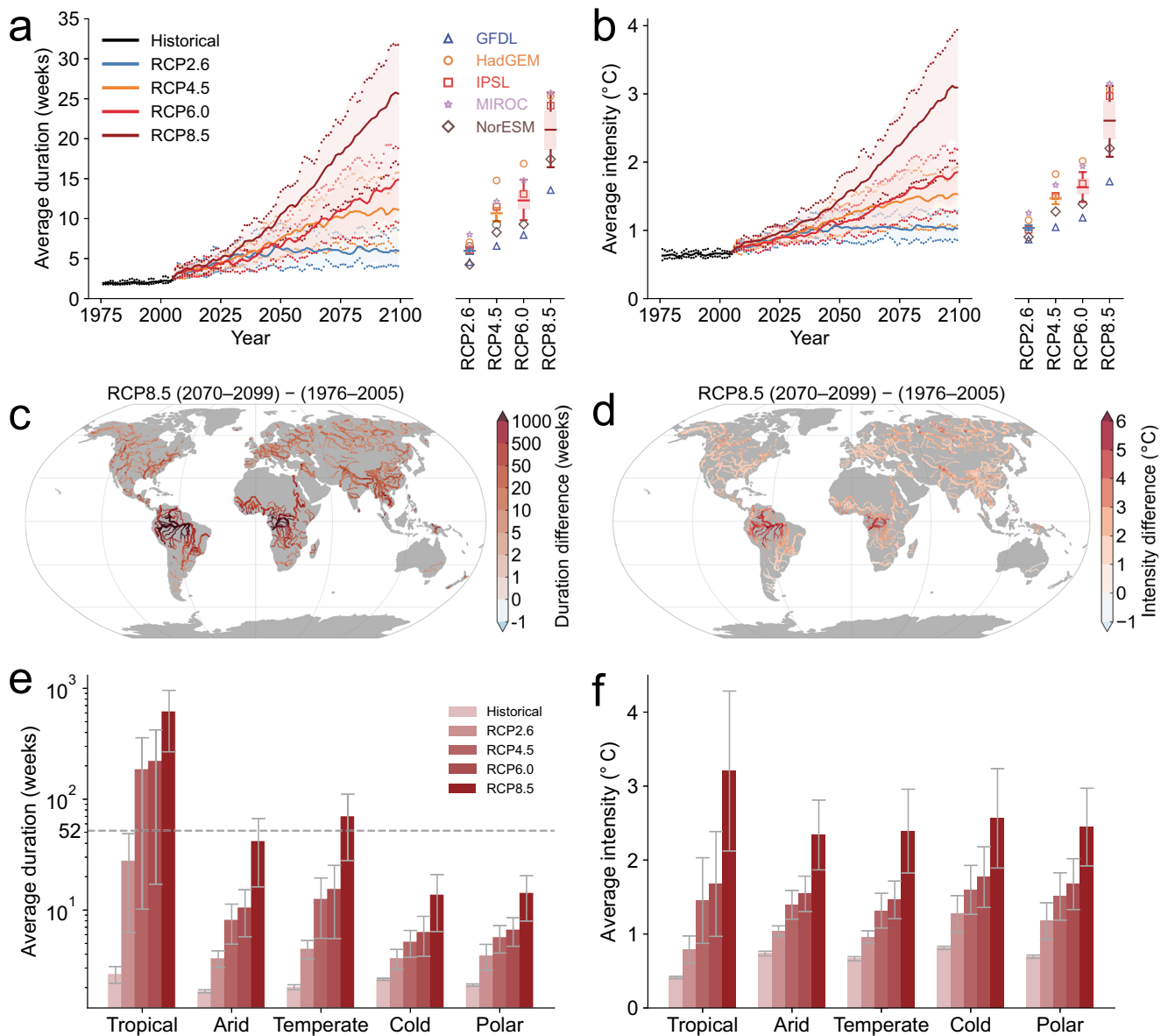


**Fig. 3 | Projected changes in river heatwaves.** Temporal evolution of simulated river heatwave duration (a) and intensity (b) under historical (1976–2005) and future climate change (2006–2099) under RCP 2.6, RCP 4.5, RCP 6.0, and RCP 8.5 scenarios. The bold curve represents the average across all examined rivers by multi-model ensemble simulations. The shaded area indicates the corresponding inter-model standard deviation. The dashed curve shows the inter-model spread of the simulations. The boxplot illustrates the results over the period of 2070–2099, with different symbols representing the average for each model. Changes in river

heatwave duration (c) and intensity (d) in the future period (2070–2099) under RCP 8.5 relative to the historical period (1976–2005). River heatwave duration (e; in log(10) scale) and intensity (f) under historical (1976–2005) and future climate scenarios (2070–2099) for RCP 2.6, RCP 4.5, RCP 6.0, and RCP 8.5. Bars in different colors represent climate zones, and error bars indicate the inter-model standard deviation. Basemaps in c and d are from Natural Earth (<https://www.naturalearthdata.com>).

By the end of the century (2070–2099), river heatwaves are projected to become more severe across all RCPs, relative to the historic period (Supplementary Figs. 10–12). In the future (2070–2099) under RCP 8.5, the average duration of river heatwaves is projected to reach 216.35 weeks, and the average intensity will be 2.69 °C (Supplementary Table 1). Thus, relative to the historical period, the duration of global river heatwaves is expected to increase by ~95-fold by the end of the century, and their intensity will increase by 4.2-fold. Among various emission scenarios, RCP 8.5 is projected to cause the most substantial increase in the river heatwave metrics, followed by RCP 6.0 and RCP 4.5.

In this study, river heatwaves are projected using the historical 90<sup>th</sup> percentile as a baseline. Considering that river water temperatures are expected to warm considerably in the 21<sup>st</sup> century, we evaluate the influence of mean river temperature change on river heatwaves by

repeating our analyses after removing the long-term warming trend (Supplementary Fig. 13). The detrended river water temperatures still lead to a projected increase in the intensity and duration of river heatwaves by the end of the 21<sup>st</sup> century under RCP 8.5. However, these changes are largely reduced compared with those calculated from the original temperature series, that is, when the warming trend is included. We note that the choice of fixed or sliding baseline for detecting river heatwaves depends on the application and should be considered by future studies. A fixed baseline is more appropriate for understanding impacts on species that adapt slowly (such as at evolutionary timescales), for example, to identify how river heatwaves may affect local species/ecosystems in the future; whereas, if species can rapidly adapt (such as at decadal timescales) to changing temperature, then a sliding baseline might be more applicable.

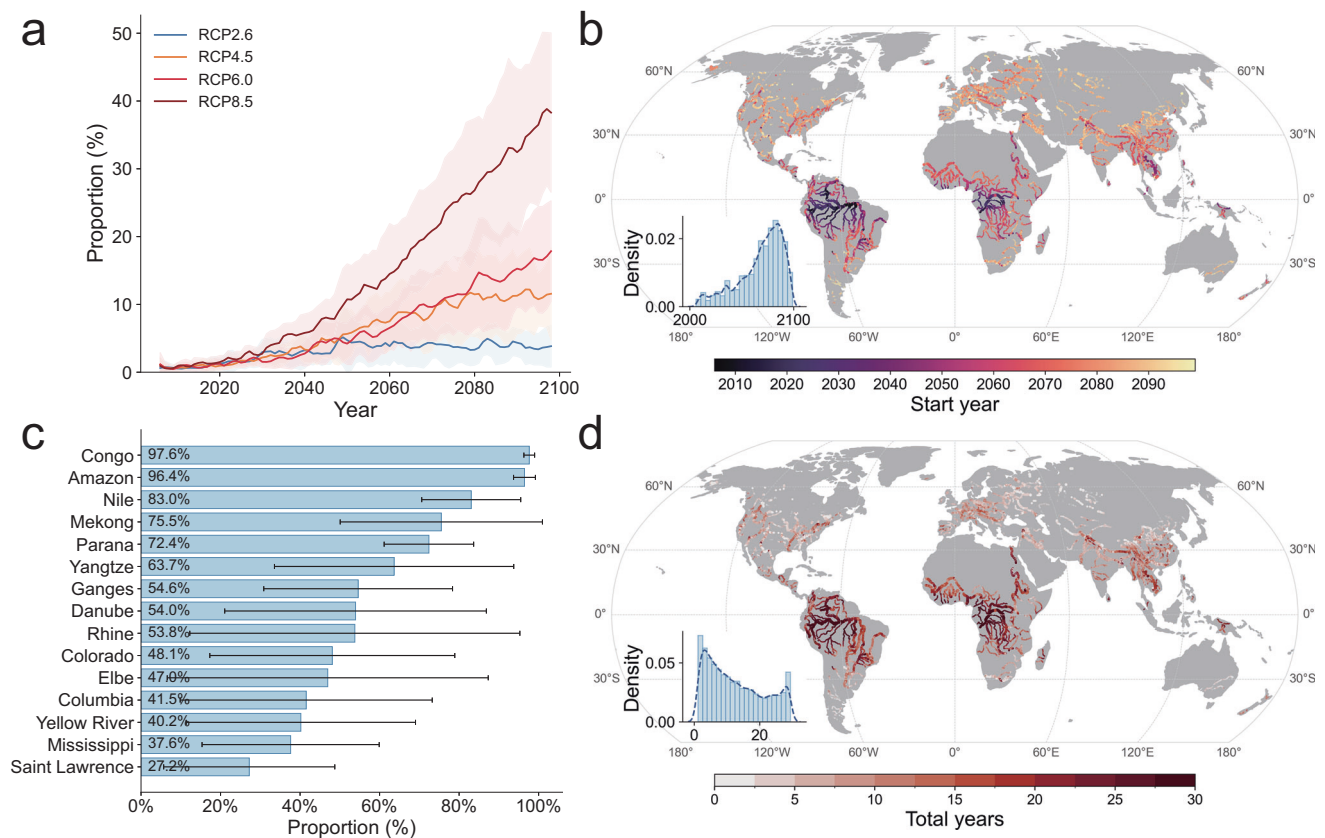


**Fig. 4 | Emergence of persistent year-round river heatwaves. a** The proportion of the examined rivers experiencing persistent year-round river heatwave state under RCP 2.6, RCP 4.5, RCP 6.0, and RCP 8.5. The shaded area indicates the corresponding inter-model standard deviation. **b** The spatial distribution of the median starting year of year-round heatwaves projected by the multi-model ensemble under RCP 8.5, with its density distribution shown in the embedded chart. **c** The

proportion of river area experiencing year-round heatwave state to the total river area in major river basins under RCP 8.5, and error bars indicate the inter-model standard deviation. **d** The number of years with year-round heatwave state in different rivers in the far future period (2070–2099) under RCP 8.5, with its density distribution shown in the embedded chart. Basemaps in **b** and **d** are from Natural Earth (<https://www.naturalearthdata.com>).

Our analysis suggests that the river heatwave intensification based on a fixed baseline exhibits considerable regional differences (Fig. 3c–d, Supplementary Figs. 10–12, and Supplementary Tables 2–5). By the end of the 21<sup>st</sup> century (2070–2099) under all four RCPs, the severity of river heatwaves is projected to increase in most rivers worldwide (Supplementary Fig. 10). These increases are particularly pronounced in Africa, South America, Eastern Europe, and North America. Tropical rivers in Africa and South America are expected to experience the most intense heatwaves. For example, the average duration of river heatwaves in the Amazon River Basin is projected to increase 358-fold from 3.21 weeks to 1150.44 weeks, with the intensity increasing 8-fold from 0.35 °C to 4.23 °C. Similarly, the average duration of river heatwaves in the Congo Basin is projected to increase from 2.47 weeks to 786.07 weeks (a ~318-fold increase), with the intensity rising from 0.39 °C to 3.43 °C (a ~9-fold increase; Supplementary Figs. 10–12).

Future projections also suggest varying magnitudes of increasing trends across different climate zones and basins (Fig. 3e–f and Supplementary Tables 3–5). Among different climate zones, the tropical zone is expected to experience the highest intensity of river heatwaves, reaching 3.21 °C in 2070–2099 under RCP 8.5, followed by rivers in cold climate zones (2.57 °C). During 2070–2099, tropical rivers will experience the longest heatwave duration, with an average of 621.23 weeks, which is ~41 times of that estimated in the cold zone (14.95 weeks). Under RCP 2.6, the global average intensity of river heatwaves will be limited to 1.01 °C, and the average duration will be 11.20 weeks. In the tropics, the duration of river heatwaves is projected to be 27.95 weeks, with heatwave intensity projected at 0.79 °C.

### Surging persistent river heatwaves

The duration of river heatwaves is projected to increase considerably by the end of the 21<sup>st</sup> century (Fig. 3 and Supplementary Fig. 12). Under RCP 8.5, the average total duration of river heatwaves during the warm season is projected to increase most rapidly (Supplementary Fig. 14), reaching an average of 16.89 weeks by the end of the century (2070–2099). Meanwhile, river heatwaves during the cold season are also expected to lengthen to 12.53 weeks. The global mean annual total duration of river heatwaves will increase to 40.16 weeks in 2070–2099, indicating a substantial extension of river heatwaves throughout all calendar days of the year. This trend toward longer durations suggests that some rivers will enter a year-round heatwave state, which we define as when river water temperature exceeds the same baseline 90<sup>th</sup> percentile threshold continuously throughout the entire calendar year<sup>20</sup>. The proportion of rivers that reach this persistent heatwave state is expected to increase during the 21<sup>st</sup> century (Fig. 4a). By 2070–2099, we estimate that a total of 49.20% of global rivers are projected to reach a year-round heatwave state (Supplementary Table 7).

Tropical rivers, which support a rich ecological diversity, are particularly vulnerable to the impacts of increasing water temperatures. In low latitudes, the persistence of river heatwaves is more pronounced, and areas that enter a year-round heatwave earlier tend to experience longer durations (Fig. 4b and Supplementary Tables 6–9). Many rivers (e.g., Congo and the Amazon) are expected to experience a year-round heatwave state for more than 20 out of 30 years in the future (Fig. 4d). The Congo River basin is the most covered (97.64% of its area) by a year-round heatwave state, followed by the

Amazon basin (96.44%) (Fig. 4c). Additionally, rivers with larger flow and depth typically exhibit longer heatwave duration. Their greater thermal inertia increases their resistance to short-term climate fluctuations but also limits their ability to recover quickly from extreme conditions, which collectively lead to a more persistent and even year-round heatwave state. We examine the top ten countries ranked by the proportion of river area under a year-round heatwave state under different emission scenarios (Supplementary Table 9). Under RCP 8.5, rivers in parts of Guyana, Congo, D.R. Congo, Gabon and Burundi are projected to experience nearly 100% year-round heatwave state by 2070–2099. Notably, even under the low emission scenario of RCP 2.6, more than half of the rivers in Congo (65.08%) and Gabon (56.82%) are projected to enter a year-round heatwave state. While these countries have relatively low population densities, they are highly dependent on their extensive river networks.

Worldwide surges of persistent river heatwaves suggest that “extremes” in the traditional perspective that have influenced rivers in the past periods will no longer be “extreme”. This surge may emerge as agents of disturbance to riverine ecosystems in the future, which has already been reported for atmospheric, marine, and lake heatwaves<sup>12–15,17,18</sup>. With the “new norm” of a possible year-round heatwave state, some rivers (or parts of them) may no longer provide livable environments for certain species (such as salmon fishes), organisms, and even ecosystems<sup>25,33–36</sup>, and the riverine ecosystems that emerge might not operate and respond to warmer waters in ways that can be expected<sup>25</sup>. The proportion of the examined rivers that experience a year-round heatwave state would be substantially reduced if low-emission scenarios such as RCPs 4.5 or 2.6 are achieved (Supplementary Table 7). For example, the global percentage of year-round heatwave state will be limited to 20.82% in 2070–2099 under RCP 4.5 (which is only one third of that under RCP 8.5) and 9.32% under RCP 2.6 (which is around one ninth of that under RCP 8.5).

### Future population exposure to river heatwaves

In addition to increasing heat hazards faced by river ecosystems, river heatwaves can also pose increasing exposure risks for humans (Fig. 5). The population exposure is calculated as the product of annual total river heatwave weeks and the population count in the same grid cell (having a unit of person-weeks; see Methods), which is likely to be directly affected by river heatwave events through the impacts on water drinking, fisheries, and agricultural management. By the middle of the 21<sup>st</sup> century under SSP1-RCP2.6, we project that global annual population exposure to river heatwaves will increase to 7.2 billion person-weeks (Fig. 5b). This exposure is more than double of that estimated in 2010 (3.5 billion person-weeks). Although river heatwaves are expected to increase relatively modestly under SSP1, population exposure is expected to decline by the end of the century, as the population structure under SSP1 is anticipated to peak and then decrease. In contrast, under SSP5-RCP8.5, annual population exposure will increase at a rate of 1.9 billion person-weeks per decade ( $p$ -value < 0.01) and is expected to reach 16.8 billion person-weeks by the end of the century. This increase is notably greater than that under the lower emission scenarios.

Considering the uneven distribution of river heatwaves and the varying abilities of countries to mitigate extreme events<sup>37,38</sup>, we assess regional disparities in population exposure to river heatwaves (Fig. 5 and Supplementary Tables 10–11). Our analysis of the top ten countries in terms of the highest population exposure by the 2090s suggests that hotspots of exposure are typically concentrated in densely populated regions, such as western Europe, eastern China, northern India, and central Africa (Fig. 5a and Supplementary Table 11). Under SSP5-RCP8.5, India is expected to face an annual population exposure of 3.1 billion person-weeks, largely due to its rapid population growth during the 21<sup>st</sup> century. The assessment of population exposure across major river basins indicates that the Ganges, Nile, Yangtze, Mississippi,

and Congo rivers are projected to have the highest population exposure in the future (Fig. 5c and Supplementary Table 10). The Ganges Basin alone is expected to face -1.7 billion person-weeks of population exposure. The increasing population exposure in these regions highlights not only the extended duration of heatwaves but also their vulnerability to adapting to climate change. These results suggest that river heatwaves will have profound impacts globally, affecting both densely populated developed regions and economically underdeveloped areas alike. Our findings also highlight the disproportionate burden of river heatwaves on densely populated regions, emphasizing the urgent need for targeted mitigation and adaptation strategies to cope with increasing threats posed by these events.

We further evaluate the population exposure of countries with different income levels (Fig. 5d). The results indicate that middle-income countries generally face the lowest exposure risks, while low-income countries experience the highest exposure, making them most vulnerable to river heatwaves. This elevated risk in low-income countries is likely due to their higher population densities. For example, under SSP5-RCP8.5 in the 2090, the population exposure in India and low-income Sub-Saharan Africa is projected to reach 3.1 billion person-weeks and 2.4 billion person-weeks, respectively. The total population exposure in the EU15 countries and the United States under SSP5-RCP8.5 is projected to reach 2.1 billion person-weeks and 1.4 billion person-weeks, respectively. Although middle-income countries typically experience lower per-grid-cell exposure, countries such as China exhibit relatively high total exposure, reaching 2.3 billion person-weeks. Additionally, population exposure in some low-income countries under SSP4-RCP6.0 surpasses that under SSP5-RCP8.5, likely due to higher population growth projections under SSP4.

### Discussion

In this study, we provide a comprehensive global assessment of river heatwaves under past and future climate change. Our assessment suggests that the frequency, duration, and intensity of river heatwaves have increased since the 1970s and will further intensify by the end of the 21<sup>st</sup> century, particularly in the Congo and Amazon basins. These intensifications of river heatwaves have profound implications for socioeconomic systems<sup>4,39</sup>, populations<sup>10,25</sup>, and ecosystems<sup>7,25,40</sup>. The extent of these intensifications will largely depend on the emission pathway followed. River heatwave increases are even more severe and persistent under the high-emission scenario (RCP 8.5), with the average duration of river heatwaves expected to exceed 216.35 weeks, far surpassing historical levels. In contrast, under low emission scenarios (RCP 2.6), while the average intensity and duration of river heatwaves increase, the change is relatively moderate. These findings suggest that reducing greenhouse gas emissions can largely mitigate the intensification of river heatwaves, thereby lessening their impacts on ecosystems and human societies.

Regional disparities in population exposure to river heatwaves will be particularly pronounced. Our results indicate that densely populated areas such as Western Europe, Eastern China, Northern India, and Central Africa will face higher exposure risks. These regions will not only experience more frequent and severe river heatwaves but also have large populations that depend heavily on river resources, making them particularly vulnerable. River resources play a crucial role in these areas, providing drinking water, agricultural irrigation, fisheries, and industrial water<sup>2–5</sup>. For example, many cities and towns depend on river infrastructure for energy production (such as hydro-power or nuclear power stations equipped with cooling towers)<sup>4,39</sup>. The increase in river water temperature and deterioration in water quality caused by river heatwaves will likely impact the effectiveness of power generation and threaten local residents' health, food security, and economic stability. Although some parts of Central Africa and South America have relatively low population densities, their high dependence on river ecosystems means that the livelihoods and

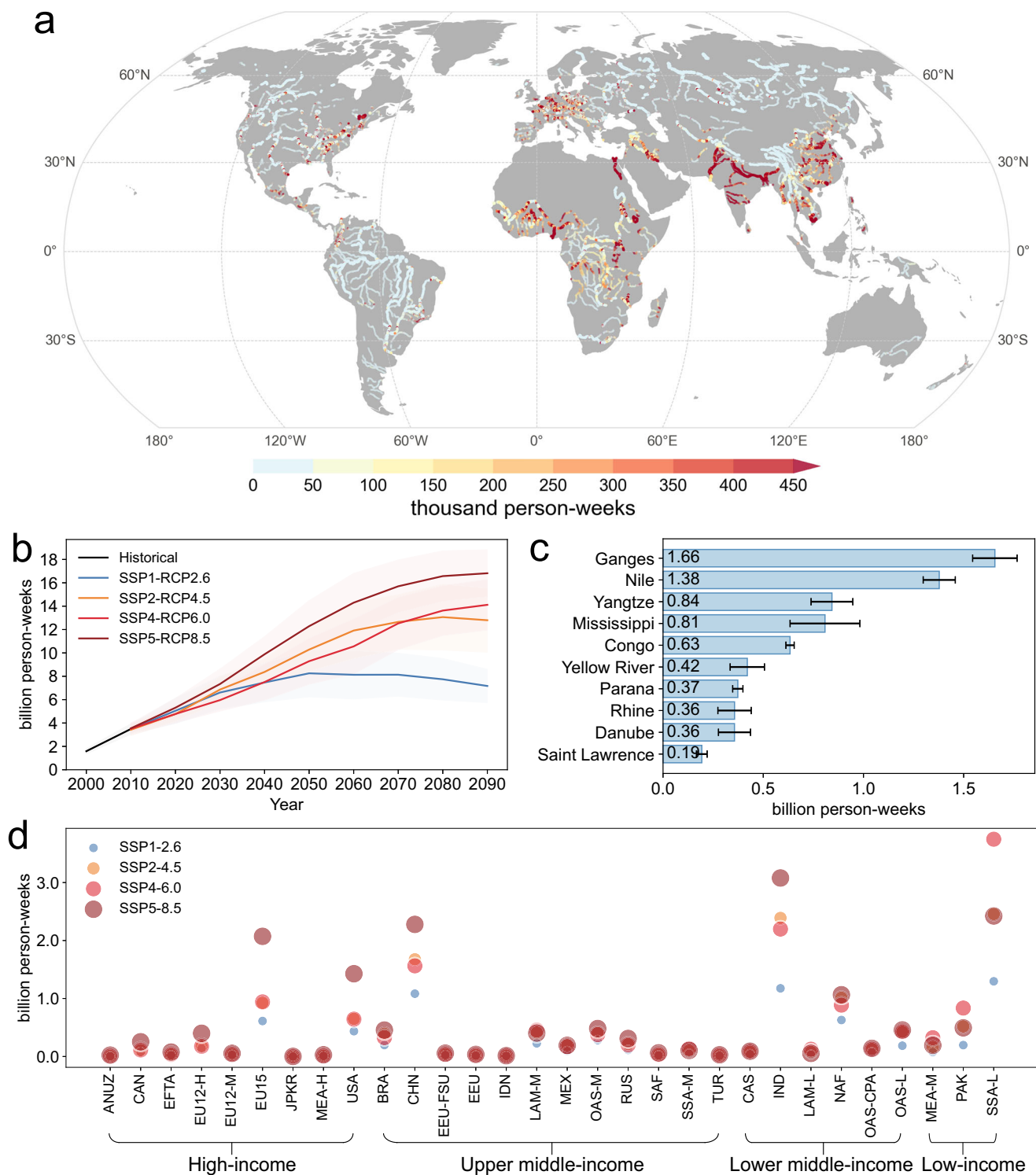


**Fig. 5 | Future population exposure to river heatwaves. a** Spatial distribution of the population exposure to river heatwaves in 2090 under SSP5-RCP8.5. **b** Temporal trends of global population exposure to river heatwaves under different scenarios, with shaded areas representing one standard deviation of the inter-model spread. **c** Ranking of population exposure in global major river basins in 2090 under SSP5-RCP8.5, and error bars indicate the inter-model standard deviation. **d** Population exposure in 2090 under SSP1-RCP2.6, SSP2-RCP4.5, SSP4-RCP6.0, and SSP5-RCP8.5 across countries with different income levels. Each data bin represents the average value over a decade (e.g., 2090 represents the average population exposure from 2086 to 2095). Basemap in a is from Natural Earth (<https://www.naturalearthdata.com>).

quality of life for residents will be severely impacted by increasing river heatwaves. Communities in these regions often rely on rivers for essential services such as agriculture, drinking water, and traditional fishing activities<sup>5,41</sup>. The intensifying effects of river heatwaves will directly disrupt these foundational activities, further exacerbating the vulnerability of communities<sup>7,39</sup>. This regional inequality in exposure underscores the differentiated impacts of global climate change on communities with varying socioeconomic backgrounds, highlighting

the need for more targeted regional responses to ensure that adaptation strategies effectively protect the most severely affected communities.

One of the most concerning projections of our study is the emergence of persistent year-round heatwave conditions in certain river basins, particularly in the Congo and Amazon basins. In the Congo Basin, over 97.6% of the basin area is expected to reach a year-round heatwave condition by the end of this century. Such persistent heatwave conditions could cause lasting and possibly irreversible damage to river ecosystems. This is a concern given that rivers have disproportionately greater biodiversity compared to other habitats<sup>42</sup> and are also among the most threatened globally<sup>43</sup>. Many freshwater species have quite narrow thermal tolerance ranges, and their core ecological functions (such as detritus decomposition) are often dominated by a limited number of functional groups, resulting in low functional redundancy. If these thermally sensitive groups are impaired, the loss of ecosystem functions or even ecological collapse may ensue<sup>25,44,45</sup>.

It is essential to recognize that river heatwaves may not be solely driven by global climate change<sup>24,46</sup>, local factors such as human activities<sup>12,47</sup> and regional hydrological characteristics<sup>26,48</sup> also play a significant role. For example, human activities can diminish the buffering capacity of river systems against thermal stress<sup>3,25,26</sup>. Disturbances such as channelization, dam construction, riparian vegetation removal, and urban development increase river exposure to solar radiation, reduce longitudinal, lateral, and vertical hydrological connectivity, and simplify habitat structures, thereby weakening the self-regulation mechanisms of ecosystems<sup>25,49</sup>. The occurrence of river heatwaves will vary depending on river flow, basin size, and human activities<sup>12,22,26</sup>. More detailed monitoring data are urgently needed to better understand the specific drivers of river heatwaves across basins, particularly in cold and tropical regions where in situ observations are extremely limited. While our research focuses on global climate change, we acknowledge that human activities, particularly in urban areas, may exacerbate temperature changes in rivers and alter local hydrological dynamics<sup>12,47</sup>.

We notice that our model simulations tend to yield longer heatwave durations and larger intensities compared to the in situ observations (Fig. S22), and we suggest that absolute values should be interpreted with caution, highlighting the influence of spatial scale on heatwave event detection. This discrepancy largely stems from the inherent difference in spatial representation between the datasets (i.e., in situ station observations versus grid-scale model simulations). In particular, the simulations represent grid-cell averages (typically spanning ~10 km), while the observational validation relies on local, point-scale measurements. Because spatial aggregation tends to smooth out short-term variability and dampen extremes, the detection of heatwaves in gridded data often results in events that appear longer in duration and higher in cumulative intensity compared to localized observations, as noted in similar assessments for atmospheric and marine heatwaves<sup>50,51</sup>. While the absolute values differ, the primary focus of our study is on the relative changes in river heatwave characteristics over time and across scenarios rather than the precise reproduction of observed magnitudes. This relative comparison remains robust because the same definition and detection algorithm are applied consistently to all model outputs.

Our global investigation indicates that climate change will significantly increase the intensity and duration of river heatwaves worldwide, leading to the emergence of persistent river heatwaves, particularly under high-emission scenarios. There are notable differences in river heatwave characteristics and exposure risks across different latitudes and regions, with tropical rivers being especially vulnerable to prolonged heatwaves. To mitigate these impacts, it is crucial to take early action to reduce greenhouse gas emissions and develop targeted regional adaptation strategies to protect river

ecosystems and the human communities that depend on them. Our investigation implies that changes in river heatwaves are expected to spark future studies for advancing the understanding of all possible drivers and consequences of riverine warming and its extremes in a warming climate.

## Methods

### Datasets

We utilize water temperature data from the FutureStreams dataset<sup>11</sup>, which is a global dataset of weekly average streamflow and water temperature at a spatial resolution of 5 arcminutes (~10 km at the equator). It covers historical simulations from 1976 to 2005 and future projections from 2006 to 2099 under four Representative Concentration Pathways (RCPs): RCP 2.6, RCP 4.5, RCP 6.0, and RCP 8.5. This dataset uses global hydrological and water temperature models (PCR-GLOBWB, DynWat) forced with climate data from five Earth System Models (ESMs): GFDL-ESM2M, HadGEM2-ES, IPSL-CM5A-LR, MIROC-ESM-CHEM, and NorESM1-M from the Inter-Sectoral Impact Model Intercomparison Project (ISI-MIP) collection, which have been bias-corrected based on the WATCH Forcing Data (WFD) dataset<sup>52</sup>. For each river grid cell, the model explicitly represents the largest river channel, and smaller rivers that share the same grid may either be excluded or lumped together within the larger river. The dataset has been validated to match well with observed temperatures at 358 worldwide sites ( $R^2 = 0.861$ )<sup>11,53</sup>. The PCR-GLOBWB<sup>54</sup> model is dynamically two-way coupled to the high-resolution water temperature model DynWat<sup>53</sup> to simulate water temperature and flow time series under different climate scenarios. For further details of the river temperature data, see ref. 11.

We use the river polygons from the Global Self-consistent, Hierarchical, High-resolution Geography Database (GSHHG)<sup>55</sup> to extract weekly water temperature values of global major rivers (including major rivers such as river-lakes, permanent major rivers, and additional major rivers). In some grids with low flow, the model may produce unrealistically high predictions due to strong water level fluctuations, and the water temperature values above 350 K (in these systems, rivers tend to become highly seasonal or disappear) are removed from the analyses. We exclude the grid cells that have more than 10% missing values, and for other cells with partial data gaps, missing values are linearly interpolated prior to further analysis. We apply the quantile delta mapping (QDM) method<sup>56,57</sup> to correct for potential bias in the modeled river water temperatures forced by five ESMs, by using the river water temperatures from the E2O reanalysis dataset during 1979–2005 as a climatological basis, as suggested by ref. 11. The QDM method maps the statistical differences in the simulations onto the cumulative distribution functions of the reanalysis (or observational) data<sup>56,57</sup>, and it has been widely used in the bias adjustment of climate and hydrological variables<sup>58,59</sup>.

The future population counts from 2000 to 2100 have been projected based on the Shared Socioeconomic Pathways (SSPs) and are available from the US National Center for Atmospheric Research (NCAR)<sup>60,61</sup>. These population data are available every ten years, depicting the number and distribution of the gridded population counts under five different SSPs. To match heatwave events (see below), we employ bilinear interpolation to aggregate the population data to a 5 arc-minute grid.

### River heatwave definition and metrics

A river heatwave is defined when weekly average temperature exceeds the 90<sup>th</sup> percentile threshold for the same calendar week over the 30-year baseline period from 1976 to 2005. The location-specific 90<sup>th</sup> percentile threshold is calculated using a 3-week window for each week over the baseline period (that is, a total sample of  $3 \times 30 = 90$  weeks). The 90<sup>th</sup> percentile provides an appropriate balance between extreme events and sample size in trend analysis, while considering the

significant impact that relatively moderate extreme events can have when combined. This local-varying percentile aligns with what has been widely used in detecting heatwaves in the atmosphere and ocean<sup>28,62,63</sup>. We test the sensitivity of river heatwave patterns by using different percentiles (95<sup>th</sup> and 99<sup>th</sup> percentiles; see Supplementary Figs. 15–16) and different windows (5- and 7-week windows; see Supplementary Figs. 17–19), which yield quantitatively similar means and trends globally, demonstrating the robustness of our results. In this study, we use weekly mean river water temperatures instead of daily data, which have been used to define atmospheric heatwaves<sup>15,16</sup>, because long-term daily river water temperature data are very limited in both reanalysis products and in situ observations. It is also noted that both daily and monthly data have been used in the literature to define marine heatwaves<sup>17,64</sup>. Further investigation can be conducted if a global daily river water temperature dataset with in situ observations of water temperature, as opposed to modeled estimates, is developed.

We examine three metrics of river heatwaves: average intensity, average duration, and occurrence frequency. The intensity of an individual river heatwave event is defined as the average temperature exceedance relative to the 90<sup>th</sup> percentile threshold over all weeks of the event, and the duration of a river heatwave is defined as the consecutive number of weeks constituting the event. For each forcing scenario, we first derive the heatwave metrics from each ESM and then average these metrics across all models to obtain a multi-model ensemble mean to reduce uncertainties arising from model differences<sup>11,65</sup>. The seasons during which river heatwaves occur are also examined. In particular, we investigate river heatwaves in two typical seasons: the extended summer and extended winter seasons. The extended summer season is defined as May–September for the Northern Hemisphere and November–March for the Southern Hemisphere, while the extended winter season is defined as November–March for the Northern Hemisphere and May–September for the Southern Hemisphere. We note that river heatwaves in both extended summer and winter seasons show increasing trends, which are more profound under higher emission scenarios such as RCP 8.5 (Supplementary Fig. 14).

### Evaluation of simulated river heatwaves

Due to the scarcity of long-term in situ daily water temperature data at the global scale, the simulated metrics of river heatwaves worldwide cannot be directly validated against observations. Nevertheless, the ability of the ESMs in simulating river heatwaves can be evaluated by comparing the simulations with those derived from an additional reanalysis dataset, the European Union's Seventh Framework Programme (EU-FP7) Earth2Observe (E2O), which provides weekly river water temperature since 1979<sup>11,66</sup>. The evaluation of climatological river heatwave patterns shows that the E2O and FutureStreams datasets exhibit similar patterns for both the climatology and long-term trend of river heatwaves during 1979–2005 (Supplementary Figs. 20–21).

Furthermore, for a specific region, we conduct an additional evaluation of the bias-corrected simulations of weekly river water temperature and river heatwave metrics against in situ measurements from the United States Geological Survey (USGS)<sup>67</sup> (Supplementary Fig. 22). We follow the methodology in ref. 22. to preprocess the USGS data. Specifically, we exclude sites affected by tidal influences or located in lakes, discard water temperature values above 50 °C, correct negative values to zero, and retain only those sites with more than 75% valid data. For missing values, we apply linear interpolation if gaps are fewer than two days; and for longer gaps, multiple linear regression models are developed for each site using 1-km<sup>2</sup> daily climate data<sup>68</sup>, and retain the sites with a model fit of  $R^2 \geq 0.80$ <sup>22</sup>. This filtering leaves 76 USGS sites with continuous water temperature records spanning 1996 to 2023. We then compare river water temperature and river heatwave metrics between observations at these sites and simulations. There is a good agreement between the observations and simulations

of river water temperature and river heatwave metrics (Supplementary Fig. 22), demonstrating the reliability of our weekly-resolution definition and river heatwave simulations.

### Population exposure estimation

We integrate river heatwave metrics simulated under four Representative Concentration Pathway (RCP) scenarios and the population data based on four Shared Socioeconomic Pathways (SSPs). Considering the integrated impacts of socioeconomic factors and climate change, we combine RCPs with SSPs to form four scenario combinations: SSP1-RCP2.6, SSP2-RCP4.5, SSP4-RCP6.0, and SSP5-RCP8.5. For each SSP-RCP scenario, we calculate the population exposed to river heatwaves in person-weeks by multiplying the duration of river heatwaves in weeks by the exposed population count<sup>69</sup>. Specifically, for each 5 arc-minute grid cell in riverine areas, we calculate the annual total weeks of river heatwaves and multiply it by the annual population at the same grid cell to obtain the annual population exposure. The population exposure to river heatwaves is thus expressed in the unit of person-weeks (Eq. 1)<sup>69</sup>:

$$E_{i,y} = P_{i,y} \times D_{i,y} \quad (1)$$

where  $E_{i,y}$  represents the population exposure to river heatwaves at the grid cell  $i$  in year  $y$ ;  $P_{i,y}$  and  $D_{i,y}$  respectively denote the annual population count and the annual total weeks of river heatwaves at the same grid cell  $i$  in year  $y$ .

For each income-level region, the total population exposure to river heatwaves is aggregated by summing the exposure of all river grid cells located in the corresponding region. The region definition is modified from the regions used in the SSPs database (<https://tntcat.iiasa.ac.at/SspDb/dsd>)<sup>70</sup>, which includes 30 macro-regions (Supplementary Fig. 23). These regions were further categorized into four income levels: high-income, upper middle-income, lower middle-income, and low-income<sup>71</sup>.

### Statistical analyses

The characteristics of river water temperature and river heatwaves are examined based on annual time series over calendar years. The long-term trends of the annual time series are evaluated using the Theil-Sen slope estimator<sup>72</sup>, and their significance is assessed by the Mann-Kendall test method<sup>73,74</sup>. These non-parametric methods are robust to missing values and outliers, and have been widely applied in previous climate change studies<sup>22,75</sup>.

### Data availability

Weekly river/stream water temperature data are obtained from the FutureStreams and E2O dataset, available at <https://geo.public.data.uu.nl/vault-futurestreams/research-futurestreams%5B1633685642%5D/original/waterTemp/>. River vector data are sourced from the Global Self-consistent, Hierarchical, High-resolution Geography (GSHHG) dataset at <https://www.soest.hawaii.edu/pwessel/gshhg/>. Watershed boundary data are acquired from the HydroBASINS dataset at <https://www.hydrosheds.org/products/hydrobasins>. The Köppen-Geiger climate classification maps (present and future) at 1-km resolution are obtained from GloH2O at <https://www.gloh2o.org/koppen/>. The downscaled global gridded population projections at 1 km resolution are available from the US National Center for Atmospheric Research (NCAR) at <https://www.cgd.ucar.edu/sections/iam/modeling/spatial-population>. Regional classification follows a modified version of the 32-region scheme from the SSPs database: <https://tntcat.iiasa.ac.at/SspDb/dsd>.

### Code availability

All analyses were performed using Python. Codes can be assessed at <https://github.com/kTeTk/River-Heatwave>.

## References

- Battin, T. J. et al. River ecosystem metabolism and carbon biogeochemistry in a changing world. *Nature* **613**, 449–459 (2023).
- Ouellet, V. et al. River temperature research and practice: Recent challenges and emerging opportunities for managing thermal habitat conditions in stream ecosystems. *Sci. Total Environ.* **736**, 139679 (2020).
- Ficklin, D. L. et al. Rethinking river water temperature in a changing, human-dominated world. *Nat. Water* **1**, 125–128 (2023).
- van Vliet, M. T. H. et al. Vulnerability of US and European electricity supply to climate change. *Nat. Clim. Change* **2**, 676–681 (2012).
- Brown, T. M., O'Connor, J. & Genner, M. J. Climate warming drives population trajectories of freshwater fish. *Proc. Natl. Acad. Sci. USA* **121**, e2410355121 (2024).
- McIntyre, P. B., Reidy Liermann, C. A. & Revenga, C. Linking freshwater fishery management to global food security and biodiversity conservation. *Proc. Natl. Acad. Sci. USA* **113**, 12880–12885 (2016).
- Barbarossa, V. et al. Threats of global warming to the world's freshwater fishes. *Nat. Commun.* **12**, 1701 (2021).
- Zhi, W., Ouyang, W., Shen, C. & Li, L. Temperature outweighs light and flow as the predominant control of dissolved oxygen across US rivers. *Nat. Water* **2022**, H150-0980 (2022).
- Tassone, S. J., Kelly, M. C., Beidler, O. N., Pace, M. L. & Marcarelli, A. M. Impacts of riverine heatwaves on rates of ecosystem metabolism in the United States. *Limnol. Oceanogr. Lett.* **10**, 464–472 (2025).
- Delpla, I., Jung, A.-V., Baures, E., Clement, M. & Thomas, O. Impacts of climate change on surface water quality in relation to drinking water production. *Environ. Int.* **35**, 1225–1233 (2009).
- Bosmans, J. et al. FutureStreams, a global dataset of future streamflow and water temperature. *Sci. Data* **9**, 307 (2022).
- Liu, S. et al. Global river water warming due to climate change and anthropogenic heat emission. *Glob. Planet. Change* **193**, 103289 (2020).
- Sun, J. et al. Long-term daily water temperatures unveil escalating water warming and intensifying heatwaves in the Odra river Basin, Central Europe. *Geosci. Front.* **15**, 101916 (2024).
- Domeisen, D. I. V. et al. Prediction and projection of heatwaves. *Nat. Rev. Earth Environ.* **4**, 36–50 (2023).
- Meehl, G. A. & Tebaldi, C. More intense, more frequent, and longer lasting heat waves in the 21st century. *Science* **305**, 994–997 (2004).
- Luo, M. et al. Anthropogenic forcing has increased the risk of longer-traveling and slower-moving large contiguous heatwaves. *Sci. Adv.* **10**, ead11598 (2024).
- Frölicher, T. L., Fischer, E. M. & Gruber, N. Marine heatwaves under global warming. *Nature* **560**, 360–364 (2018).
- Zhang, Y., Du, Y., Feng, M. & Hobday, A. J. Vertical structures of marine heatwaves. *Nat. Commun.* **14**, 6483 (2023).
- Wang, X. et al. Climate change drives rapid warming and increasing heatwaves of lakes. *Sci. Bull.* **68**, 1574–1584 (2023).
- Woolway, R. I. et al. Lake heatwaves under climate change. *Nature* **589**, 402–407 (2021).
- van Vliet, M. T. H. et al. Global river discharge and water temperature under climate change. *Glob. Environ. Change* **23**, 450–464 (2013).
- Tassone, S. J. et al. Increasing heatwave frequency in streams and rivers of the United States. *Limnol. Oceanogr. Lett.* **8**, 295–304 (2023).
- Zhou, Q. et al. Characteristics of river heatwaves in the Vistula River basin, Europe. *Heliyon* **10**, e35987 (2024).
- van Vliet, M. T. H., Ludwig, F., Zwolsman, J. J. G., Weedon, G. P. & Kabat, P. Global river temperatures and sensitivity to atmospheric warming and changes in river flow. *Water Resour. Res.* **47**, 2 (2011).
- Johnson, M. F. et al. Rising water temperature in rivers: ecological impacts and future resilience. *WIREs Water* **11**, e1724 (2024).
- Caissie, D. The thermal regime of rivers: a review. *Freshw. Biol.* **51**, 1389–1406 (2006).
- He, Y. et al. Arctic Amplification of marine heatwaves under global warming. *Nat. Commun.* **15**, 8265 (2024).
- Oliver, E. C. J. et al. Longer and more frequent marine heatwaves over the past century. *Nat. Commun.* **9**, 1324 (2018).
- Li, X., Zhao, L., Wang, S., Cheng, X. & Wang, L. Unstable permafrost regions experience more severe heatwaves in a warming climate. *npj Clim. Atmos. Sci.* **8**, 147 (2025).
- Davy, R. & Griewank, P. Arctic amplification has already peaked. *Environ. Res. Lett.* **18**, 084003 (2023).
- Previdi, M., Smith, K. L. & Polvani, L. M. Arctic amplification of climate change: a review of underlying mechanisms. *Environ. Res. Lett.* **16**, 093003 (2021).
- Dai, A., Luo, D., Song, M. & Liu, J. Arctic amplification is caused by sea-ice loss under increasing CO<sub>2</sub>. *Nat. Commun.* **10**, 121 (2019).
- Crozier, L. G. et al. Snake River sockeye and Chinook salmon in a changing climate: Implications for upstream migration survival during recent extreme and future climates. *PLoS ONE* **15**, e0238886 (2020).
- Jeffries, K. M. et al. Consequences of high temperatures and premature mortality on the transcriptome and blood physiology of wild adult sockeye salmon (*Oncorhynchus nerka*). *Ecol. Evol.* **2**, 1747–1764 (2012).
- Westley, P. A. H. Documentation of en route mortality of summer chum salmon in the Koyukuk River, Alaska and its potential linkage to the heatwave of 2019. *Ecol. Evol.* **10**, 10296–10304 (2020).
- Isaak, D. J., Wollrab, S., Horan, D. & Chandler, G. Climate change effects on stream and river temperatures across the northwest U.S. from 1980–2009 and implications for salmonid fishes. *Clim. Change* **113**, 499–524 (2012).
- Carleton, T. A. & Hsiang, S. M. Social and economic impacts of climate. *Science* **353**, aad9837 (2016).
- Kc, S. & Lutz, W. The human core of the shared socioeconomic pathways: Population scenarios by age, sex and level of education for all countries to 2100. *Glob. Environ. Change* **42**, 181–192 (2017).
- Allison, E. H. et al. Vulnerability of national economies to the impacts of climate change on fisheries. *Fish. Fish.* **10**, 173–196 (2009).
- Mouthon, J. & Daufresne, M. Effects of the 2003 heatwave and climatic warming on mollusc communities of the Saône: a large lowland river and of its two main tributaries (France). *Glob. Change Biol.* **12**, 441–449 (2006).
- Vörösmarty, C. J. et al. Global threats to human water security and river biodiversity. *Nature* **467**, 555–561 (2010).
- Reid, A. J. et al. Emerging threats and persistent conservation challenges for freshwater biodiversity. *Biol. Rev.* **94**, 849–873 (2019).
- Dudgeon, D. et al. Freshwater biodiversity: importance, threats, status and conservation challenges. *Biol. Rev.* **81**, 163–182 (2006).
- Pyne, M. I. & Poff, N. L. Vulnerability of stream community composition and function to projected thermal warming and hydrologic change across ecoregions in the western United States. *Glob. Change Biol.* **23**, 77–93 (2017).
- Statzner, B. & Bêche, L. A. Can biological invertebrate traits resolve effects of multiple stressors on running water ecosystems?. *Freshw. Biol.* **55**, 80–119 (2010).
- Haddeland, I. et al. Global water resources affected by human interventions and climate change. *Proc. Natl. Acad. Sci. USA* **111**, 3251–3256 (2014).
- Grey, V., Smith-Miles, K., Fletcher, T. D., Hatt, B. E. & Coleman, R. A. Empirical evidence of climate change and urbanization impacts on warming stream temperatures. *Water Res.* **247**, 120703 (2023).
- Dugdale, S., Hannah, D. & Malcolm, I. River temperature modelling: a review of process-based approaches and future directions. *Earth Sci. Rev.* **175**, 97–113 (2017).

49. Woodward, G. et al. Chapter 2 - Ecological networks in a changing climate. in *Advances in Ecological Research* (ed. Woodward, G.) vol. 42 71–138 (Academic Press, 2010).
50. Hirsch, A. L., Ridder, N. N., Perkins-Kirkpatrick, S. E. & Ukkola, A. CMIP6 multimodel evaluation of present-day heatwave attributes. *Geophys. Res. Lett.* **48**, e2021GL095161 (2021).
51. Oliver, E. C. J. et al. Projected marine heatwaves in the 21st century and the potential for ecological impact. *Front. Mar. Sci.* **6**, 481127 (2019).
52. Hempel, S., Frieler, K., Warszawski, L., Schewe, J. & Piontek, F. A trend-preserving bias correction – the ISI-MIP approach. *Earth Syst. Dyn.* **4**, 219–236 (2013).
53. Wanders, N., van Vliet, M. T. H., Wada, Y., Bierkens, M. F. P. & van Beek, L. P. H. (Rens). High-resolution global water temperature modeling. *Water Resour. Res.* **55**, 2760–2778 (2019).
54. Sutanudjaja, E. H. et al. PCR-GLOBWB 2: a 5 arcmin global hydrological and water resources model. *Geosci. Model Dev.* **11**, 2429–2453 (2018).
55. Wessel, P. & Smith, W. H. F. A global, self-consistent, hierarchical, high-resolution shoreline database. *J. Geophys. Res. Solid Earth* **101**, 8741–8743 (1996).
56. Tong, Y. et al. Bias correction of temperature and precipitation over China for RCM simulations using the QM and QDM methods. *Clim. Dyn.* **57**, 1425–1443 (2021).
57. Cannon, A. J., Sobie, S. R. & Murdock, T. Q. Bias correction of GCM precipitation by quantile mapping: How well do methods preserve changes in quantiles and extremes?. *J. Clim.* **28**, 6938–6959 (2015).
58. Ansari, R., Casanueva, A., Liaqat, M. U. & Grossi, G. Evaluation of bias correction methods for a multivariate drought index: case study of the Upper Jhelum Basin. *Geosci. Model Dev.* **16**, 2055–2076 (2023).
59. Ravinandrasana, V. P. & Franzke, C. L. E. The first emergence of unprecedented global water scarcity in the Anthropocene. *Nat. Commun.* **16**, 8281 (2025).
60. Gao, J. Downscaling global spatial population projections from 1/8-degree to 1-km grid cells. <https://doi.org/10.5065/D60Z721H> (2017).
61. Jones, B. & O'Neill, B. C. Spatially explicit global population scenarios consistent with the Shared Socioeconomic Pathways. *Environ. Res. Lett.* **11**, 084003 (2016).
62. Hobday, A. J. et al. A hierarchical approach to defining marine heatwaves. *Prog. Oceanogr.* **141**, 227–238 (2016).
63. Smale, D. A. et al. Marine heatwaves threaten global biodiversity and the provision of ecosystem services. *Nat. Clim. Chang.* **9**, 306–312 (2019).
64. Jacox, M. G., Alexander, M. A., Bograd, S. J. & Scott, J. D. Thermal displacement by marine heatwaves. *Nature* **584**, 82–86 (2020).
65. Kundzewicz, Z. W. et al. Uncertainty in climate change impacts on water resources. *Environ. Sci. Policy* **79**, 1–8 (2018).
66. Weedon, G. P. et al. The WFDEI meteorological forcing data set: WATCH forcing data methodology applied to ERA-Interim reanalysis data. *Water Resour. Res.* **50**, 7505–7514 (2014).
67. Survey, U. G. National water information system data available on the World Wide Web (USGS water data for the nation, 2016).
68. Thornton, M. M., Shrestha, R., Wei, Y., Thornton, P. E. & Kao, S.-C. Daymet: Daily Surface Weather Data on a 1-km Grid for North America, Version 4. <https://doi.org/10.3334/ORNLDAC/1840> (2020).
69. Jones, B. et al. Future population exposure to US heat extremes. *Nat. Clim. Change* **5**, 652–655 (2015).
70. Chen, M. et al. Rising vulnerability of compound risk inequality to ageing and extreme heatwave exposure in global cities. *npj Urban Sustain* **3**, 1–11 (2023).
71. Wu, S. et al. Rapid flips between warm and cold extremes in a warming world. *Nat. Commun.* **16**, 3543 (2025).
72. Sen, P. K. Estimates of the regression coefficient based on Kendall's Tau. *J. Am. Stat. Assoc.* **63**, 1379–1389 (1968).
73. Mann, H. B. Nonparametric tests against trend. *Econometrica* **13**, 245–259 (1945).
74. Kendall, M. G. *Rank Correlation Methods* (Griffin, 1948).
75. Kaushal, S. S. et al. Rising stream and river temperatures in the United States. *Front. Ecol. Environ.* **8**, 461–466 (2010).

## Acknowledgements

This study was funded by the National Natural Science Foundation of China (No. 42371028). R.I.W. was supported by a UKRI Natural Environment Research Council (NERC) Independent Research Fellowship (No. NE/T011246/1). The authors are grateful to three reviewers whose constructive comments have greatly improved the paper.

## Author contributions

M.L. initiated and designed the study. Y.C., N.W. and Z.S. compiled the data. Y.C. and Z.S. performed the analyses. Y.C. and Z.S. drafted the manuscript, with help from M.L. M.L., Y.C., Z.S., R.I.W., N.W., S.W., and Z.H. contributed to the result discussion and the review and editing of the manuscript.

## Competing interests

The authors declare no competing interests.

## Additional information

**Supplementary information** The online version contains supplementary material available at <https://doi.org/10.1038/s41467-025-66868-5>.

**Correspondence** and requests for materials should be addressed to Ming Luo.

**Peer review information** *Nature Communications* thanks the anonymous reviewers for their contribution to the peer review of this work. A peer review file is available.

**Reprints and permissions information** is available at <http://www.nature.com/reprints>

**Publisher's note** Springer Nature remains neutral with regard to jurisdictional claims in published maps and institutional affiliations.

**Open Access** This article is licensed under a Creative Commons Attribution-NonCommercial-NoDerivatives 4.0 International License, which permits any non-commercial use, sharing, distribution and reproduction in any medium or format, as long as you give appropriate credit to the original author(s) and the source, provide a link to the Creative Commons licence, and indicate if you modified the licensed material. You do not have permission under this licence to share adapted material derived from this article or parts of it. The images or other third party material in this article are included in the article's Creative Commons licence, unless indicated otherwise in a credit line to the material. If material is not included in the article's Creative Commons licence and your intended use is not permitted by statutory regulation or exceeds the permitted use, you will need to obtain permission directly from the copyright holder. To view a copy of this licence, visit <http://creativecommons.org/licenses/by-nc-nd/4.0/>.

© The Author(s) 2025